



Universiteit
Leiden
The Netherlands

Dirac and Majorana edge states in graphene and topological superconductors

Akhmerov, A.R.

Citation

Akhmerov, A. R. (2011, May 31). *Dirac and Majorana edge states in graphene and topological superconductors*. *Casimir PhD Series*. Retrieved from <https://hdl.handle.net/1887/17678>

Version: Not Applicable (or Unknown)
License: [Leiden University Non-exclusive license](#)
Downloaded from: <https://hdl.handle.net/1887/17678>

Note: To cite this publication please use the final published version (if applicable).

Chapter 9

Domain wall in a chiral p -wave superconductor: a pathway for electrical current

9.1 Introduction

Chiral edge states are gapless excitations at the boundary of a two-dimensional system that can propagate in only a single direction. They appear prominently in the quantum Hall effect [185, 186]: The absence of backscattering in a chiral edge state explains the robustness of the quantization of the Hall conductance against disorder. Analogous phenomena in a superconductor with broken time reversal symmetry are known as the spin quantum Hall effect [6, 7, 187] and the thermal quantum Hall effect [188, 189], in reference to the transport of spin and heat along chiral edge states.

Unlike the original (electrical) quantum Hall effect, both these superconducting analogues have eluded observation, which is understandable since it is so much more difficult to measure spin and heat transport than electrical transport. Proposals to detect chiral edge states in a superconductor through their equilibrium magnetization are hindered by screening currents in the bulk, which cancel the magnetic field (Meissner effect) [190–193].

Here we show that the boundary between domains of opposite chirality ($p_x \pm ip_y$) in a chiral p -wave superconductor forms a one-way channel for electrical charge, in much the same way as edge states in the quantum Hall effect. This is not an immediate consequence of chirality: Since the charge of excitations in a superconductor is only conserved modulo the Cooper pair charge of $2e$, the absence of backscattering in a superconducting chiral edge state does not imply conservation of the electrical current. Indeed, one chiral edge state within a single domain has zero conductance due to electron-hole symmetry. We calculate the conductance of the domain wall, measured between a pair of metal contacts at the two ends (see Fig. 9.1), and find that it is nonzero, regardless of the separation of the contacts.

Our analysis is generally applicable to so-called class-D topological superconduct-

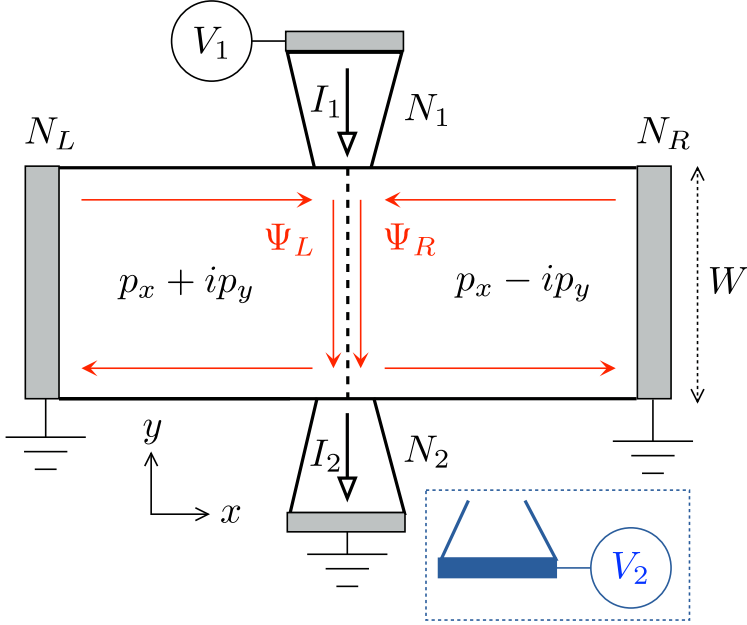


Figure 9.1: Superconducting strip divided by a domain wall (dashed line, length W) into domains with $p_x \pm ip_y$ symmetry. The edge states Ψ_L, Ψ_R of opposite chirality in the two domains are indicated by red arrows. These unpaired Majorana modes can carry heat current between contacts N_L and N_R , but no electrical current. A normal metal electrode N_1 at voltage V_1 injects charge into the domain wall, which is detected as an electrical current I_2 at the other end N_2 . In an alternative measurement configuration (indicated in blue), contact N_2 measures a voltage V_2 without drawing a current.

tors [12, 194], characterized by the presence of electron-hole symmetry and the absence of both time-reversal and spin-rotation symmetry. It can be applied to the various realizations of chiral p -wave superconductors proposed in the literature (strontium ruthenate [193], superfluids of fermionic cold atoms [148, 195], and ferromagnet-superconductor heterostructures [131, 196]).

9.2 Calculation of transport properties

We start from the Bogoliubov-De Gennes equation,

$$\begin{pmatrix} H_0 - E_F & \Delta \\ \Delta^\dagger & -H_0^* + E_F \end{pmatrix} \begin{pmatrix} u \\ v \end{pmatrix} = E \begin{pmatrix} u \\ v \end{pmatrix}, \quad (9.1)$$

for coupled electron and hole excitations $u(\mathbf{r}), v(\mathbf{r})$ at energy E above the Fermi level E_F . The single-particle Hamiltonian is $H_0 = (\mathbf{p} + e\mathbf{A})^2/2m + U$, with $\mathbf{p} = -i\hbar\partial/\partial\mathbf{r}$

the momentum, $\mathbf{A}(\mathbf{r})$ the vector potential, and $U(\mathbf{r})$ the electrostatic potential. The dynamics is two-dimensional, so $\mathbf{r} = (x, y)$, $\mathbf{p} = (p_x, p_y)$. The pair potential Δ has the spin-polarized-triplet p -wave form [140]:

$$\Delta = (2p_F)^{-1}(\boldsymbol{\eta} \cdot \mathbf{p} + \mathbf{p} \cdot \boldsymbol{\eta}), \quad (9.2)$$

in terms of a two-component order parameter $\boldsymbol{\eta} = (\eta_x, \eta_y)$. The two chiralities $p_x \pm i p_y$ correspond to $\boldsymbol{\eta}_{\pm} = \Delta_0 e^{i\phi}(1, \pm i)$, with Δ_0 the excitation gap and ϕ the superconducting phase. Since $\Delta^\dagger = -\Delta^*$, a solution (u, v) of Eq. (9.1) at energy E is related to another solution (v^*, u^*) at energy $-E$ (electron-hole symmetry). A domain wall along $x = 0$, with a phase difference ϕ between the domains, has order parameter [197, 198]

$$\eta_x(x) = \Delta_0[e^{-i\phi/2} \cos \chi(x) + e^{i\phi/2} \sin \chi(x)], \quad (9.3a)$$

$$\eta_y(x) = i\Delta_0[e^{-i\phi/2} \cos \chi(x) - e^{i\phi/2} \sin \chi(x)], \quad (9.3b)$$

The function $\chi(x)$ increases from 0 to $\pi/2$ over a coherence length $\xi_0 = \hbar v_F / \Delta_0$ around $x = 0$.

At energies E below Δ_0 the excitations are nondegenerate chiral edge states Ψ_L and Ψ_R circulating in opposite directions in the two domains [190, 199–201]. (See Fig. 9.1.) At the domain wall the two states mix, so that an excitation entering the domain wall in the state Ψ_L^{in} or Ψ_R^{in} can exit in either of the two states Ψ_L^{out} and Ψ_R^{out} . We first analyze this edge state scattering problem between contacts N_L and N_R , and then introduce the contacts N_1 and N_2 to the domain wall.

The edge state excitations have creation operators $\boldsymbol{\gamma}^\dagger(E) = (\gamma_L^\dagger(E), \gamma_R^\dagger(E))$, which satisfy the electron-hole symmetry relation

$$\boldsymbol{\gamma}(E) = \boldsymbol{\gamma}^\dagger(-E). \quad (9.4)$$

At zero energy one has $\boldsymbol{\gamma} = \boldsymbol{\gamma}^\dagger$, so these are Majorana fermions [140]. The unitary scattering matrix $S(E)$ relates incoming and outgoing operators, $\boldsymbol{\gamma}^{\text{out}}(E) = S(E)\boldsymbol{\gamma}^{\text{in}}(E)$. Electron-hole symmetry for both $\boldsymbol{\gamma}^{\text{in}}$ and $\boldsymbol{\gamma}^{\text{out}}$ requires $S(E)\boldsymbol{\gamma}^{\text{in}}(E) = \boldsymbol{\gamma}^{\text{in}}(E)S^\dagger(-E)$, hence $S(E) = S^*(-E)$. The zero-energy scattering matrix $S(0) \equiv S_{dw}$ of the domain wall is therefore a real unitary, or orthogonal, matrix. We may parametrize it by

$$S_{dw} = \begin{pmatrix} \cos \psi & \sin \psi \\ (-1)^{p+1} \sin \psi & (-1)^p \cos \psi \end{pmatrix} = \sigma_z^p e^{i\psi\sigma_y}, \quad (9.5)$$

in terms of a mixing angle ψ and a parity index $p \in \{0, 1\}$.

The mixing angle $\psi = k_y W$ is determined by the phase accumulated by the pair of chiral Majorana modes, as they propagate with wave number $\pm k_y$ along the domain wall of length W . The dispersion relation $E(k_y)$ of the Majorana modes was calculated in Ref. [200], for a step function order parameter at $x = 0$, including also the effect of a tunnel barrier $U = U_0\delta(x)$ (tunnel probability D , zero magnetic field). By equating $E(k_y) = 0$ and solving for k_y we obtain the mixing angle

$$\psi = k_F W \sqrt{D} \cos(\phi/2). \quad (9.6)$$

The mixing angle can in principle be measured through thermal transport between contacts N_L and N_R , since the heat current through the domain wall is $\propto \sin^2 \psi$. In what follows we consider instead a purely electrical measurement of transport along the domain wall, that (as we shall see) is independent of the degree of mixing of the Majorana modes.

The measurement that we propose consists of the injection of electrons from contact N_1 at voltage V_1 (relative to the superconductor) and the detection at contact N_2 . We consider two detection schemes: In the first scheme contact N_2 is kept at the same potential as the superconductor and measures a current I_2 , leading to the nonlocal conductance $G_{12} = I_2/V_1$. In the second scheme contact N_2 is a voltage probe drawing no net current and measuring a voltage V_2 . The ratio $R_{12} = V_2/I_1$, with I_1 the current entering the superconductor through contact N_1 , is the nonlocal resistance. The two nonlocal quantities are related by $R_{12} = G_{12}/G_1G_2$, with $G_i = |I_i/V_i|$ the contact conductance of electrode N_i (measured with the other contact grounded).

We take the zero-temperature and zero-voltage limit, so that we can use the zero-energy scattering matrix to calculate the various conductances. The scattering problem at contact N_1 involves, in addition to the Majorana operators $\boldsymbol{\gamma} = (\gamma_L, \gamma_R)$, the electron and hole annihilation operators a_n and b_n in mode $n = 1, 2, \dots, N$. These are related by $b_n(E) = a_n^\dagger(-E)$. The even and odd combinations γ_n^\pm , defined by

$$\begin{pmatrix} \gamma_n^+ \\ \gamma_n^- \end{pmatrix} = u \begin{pmatrix} a_n \\ b_n \end{pmatrix}, \quad u = \sqrt{\frac{1}{2}} \begin{pmatrix} 1 & 1 \\ -i & i \end{pmatrix}, \quad (9.7)$$

satisfy the same electron-hole symmetry relation (9.4) as γ_L, γ_R , and therefore represent Majorana fermions at $E = 0$. We denote $\boldsymbol{\gamma}_n = (\gamma_n^+, \gamma_n^-)$ and collect these operators in the vector $\boldsymbol{\Gamma} = (\boldsymbol{\gamma}_1, \boldsymbol{\gamma}_2, \dots, \boldsymbol{\gamma}_N)$. The scattering matrix S_1 of contact N_1 relates incoming and outgoing operators,

$$\begin{pmatrix} \boldsymbol{\gamma} \\ \boldsymbol{\Gamma} \end{pmatrix}_{\text{out}} = S_1 \begin{pmatrix} \boldsymbol{\gamma} \\ \boldsymbol{\Gamma} \end{pmatrix}_{\text{in}}, \quad S_1 = \begin{pmatrix} r_1 & t_1 \\ t'_1 & r'_1 \end{pmatrix}. \quad (9.8)$$

Electron-hole symmetry implies that S_1 is $(2N + 2) \times (2N + 2)$ orthogonal matrix at zero energy. Similarly, the zero-energy scattering matrix S_2 of contact N_2 is a $(2N' + 2) \times (2N' + 2)$ orthogonal matrix. (The number of modes is N, N' in contacts N_1, N_2 respectively.)

The $2N' \times 2N$ transmission matrix

$$t_{21} = t'_2 S_{dw} t_1 = t'_2 \sigma_z^p e^{i\psi \sigma_y} t_1 \quad (9.9)$$

from contact N_1 to N_2 is the product of the $2 \times 2N$ submatrix t_1 of S_1 (transmission from N_1 to the domain wall), the 2×2 scattering matrix S_{dw} (transmission along the domain wall), and the $2N' \times 2$ submatrix t'_2 of S_2 (transmission from the domain wall to N_2).

The total transmission probability T_{ee} , summed over all modes, of an electron at

contact N_1 to an electron at contact N_2 is given by

$$T_{ee} = \frac{1}{4} \text{Tr} U^\dagger t_{21}^\dagger U (1 + \Sigma_z) U^\dagger t_{21} U (1 + \Sigma_z) \quad (9.10)$$

$$= \frac{1}{4} \text{Tr} t_{21}^\dagger (1 - \Sigma_y) t_{21} (1 - \Sigma_y), \quad (9.11)$$

where we have defined the direct sums $U = u \oplus u \cdots \oplus u$, $\Sigma_i = \sigma_i \oplus \sigma_i \cdots \oplus \sigma_i$ and we have used that $u \sigma_z u^\dagger = -\sigma_y$. Similarly, the total electron-to-hole transmission probability T_{he} reads

$$T_{he} = \frac{1}{4} \text{Tr} t_{21}^\dagger (1 + \Sigma_y) t_{21} (1 - \Sigma_y). \quad (9.12)$$

Since $I_2 = (e^2/h) V_1 (T_{ee} - T_{he})$, the nonlocal conductance takes the form

$$G_{12} = (e^2/h) \frac{1}{2} \text{Tr} t_{21}^T \Sigma_y t_{21} \Sigma_y. \quad (9.13)$$

We have used that $t_{21}^\dagger = t_{21}^T$ and $\text{Tr} t_{21}^T \Sigma_y t_{21} = 0$ (being the trace of an antisymmetric matrix). The nonlocal resistance can be written in a similar form upon division by the contact conductances,

$$R_{12} = \frac{G_{12}}{G_1 G_2}, \quad G_i = (e^2/h) \frac{1}{2} \text{Tr} (1 - \Sigma_y r_i'^T \Sigma_y r_i'). \quad (9.14)$$

We will henceforth set e^2/h to unity in most equations.

Substitution of Eq. (9.9) into Eq. (9.13) gives the conductance

$$G_{12} = \frac{1}{2} \text{Tr} T_1 S_{dw}^T T_2 S_{dw}, \quad (9.15)$$

in terms of the 2×2 matrices $T_1 = t_1 \Sigma_y t_1^T$, $T_2 = t_2'^T \Sigma_y t_2'$. We now use the identity

$$\text{Tr} A_1 A_2 = \frac{1}{2} (\text{Tr} A_1 \sigma_y) (\text{Tr} A_2 \sigma_y), \quad (9.16)$$

valid for any pair of 2×2 antisymmetric matrices A_1, A_2 . Taking $A_1 = T_1$, $A_2 = S_{dw}^T T_2 S_{dw}$ we arrive at

$$G_{12} = (-1)^p \alpha_1 \alpha_2, \quad \alpha_i = \frac{1}{2} \text{Tr} T_i \sigma_y, \quad (9.17a)$$

$$R_{12} = (-1)^p \beta_1 \beta_2, \quad \beta_i = \alpha_i / G_i, \quad (9.17b)$$

since $\text{Tr} S_{dw}^T T_2 S_{dw} \sigma_y = (-1)^p \text{Tr} T_2 \sigma_y$ in view of Eq. (9.5).

Eq. (9.17) expresses the nonlocal conductance and resistance in terms of the scattering matrices S_1, S_2 of the two contacts N_1, N_2 . The scattering matrix S_{dw} of the domain wall enters only through the parity index p , and not through the mixing angle ψ . That the transferred charge depends only on a parity index is a generic feature of a single-mode scattering problem with class D symmetry [144, 145, 202–204]. Quite generally, p counts the number (modulo 2) of zero-energy bound states, which in our case would be trapped in vortices in the domain wall.

A measurement of the domain wall conductance would have several characteristic features: Most prominently, the conductance is zero unless both contacts N_1 and N_2 are at the domain wall; if at least one contact is moved away from the domain wall, the conductance vanishes because a single Majorana edge mode cannot carry an electrical current at the Fermi level.¹ This feature would distinguish chiral p -wave superconductors (symmetry class D) from chiral d -wave superconductors (symmetry class C), where the Majorana edge modes come in pairs and can carry a current. The chirality itself can be detected by interchanging the injecting and detecting contacts: only one choice can give a nonzero conductance. While vortices trapped in the domain wall can change the sign of the conductance (through the parity index p), other properties of the domain wall have no effect on G_{12} . In particular, there is no dependence on the length W .

To illustrate these features in a model calculation, we consider the case of two single-mode contacts ($N = N' = 1$) coupled to the domain wall through a disordered interface. We model the effect of disorder using random contact scattering matrices S_1 and S_2 , drawn independently with a uniform distribution from the ensemble of 4×4 orthogonal matrices. In the context of random-matrix theory [121], uniformly distributed ensembles of unitary matrices are called “circular”, so our ensemble could be called the “circular real ensemble” (CRE) — to distinguish it from the usual circular unitary ensemble (CUE) of complex unitary matrices.²

Using the expression for the uniform measure on the orthogonal group [204] (see also App. 9.A), we obtain the distributions of the parameters α_i and β_i characterizing contact N_i :

$$P(\alpha) = 1 - |\alpha|, \quad P(\beta) = (1 + |\beta|)^{-2}, \quad |\alpha|, |\beta| \leq 1. \quad (9.18)$$

The distribution of the nonlocal conductance $G_{12} = (-1)^p \alpha_1 \alpha_2$, plotted in Fig. 9.2, then follows from

$$\begin{aligned} P(G_{12}) &= \int_{-1}^1 d\alpha_1 \int_{-1}^1 d\alpha_2 \delta(G_{12} - \alpha_1 \alpha_2) P(\alpha_1) P(\alpha_2) \\ &= 4|G_{12}| - 4 - 2(1 + |G_{12}|) \ln |G_{12}|, \quad |G_{12}| < 1. \end{aligned} \quad (9.19)$$

(There is no dependence on the parity index p because P is symmetric around zero.) The distribution of the nonlocal resistance $R_{12} = (-1)^p \beta_1 \beta_2$ follows similarly and as we can see in Fig. 9.2 it lies close to $P(G_{12})$.

The difference between the two quantities G_{12} and R_{12} becomes important if the contacts between the metal and the superconductor contain a tunnel barrier. A tunnel barrier suppresses G_{12} but has no effect on R_{12} . More precisely (for more details see App. 9.B), any series resistance in the single-mode contacts N_1 and N_2 which does not

¹That the nonlocal conductance vanishes if one of the two contacts couples only to a single domain, can be seen directly from Eq. (9.17): If, say, contact 1 couples only to the right domain, then only the 2, 2 element of T_1 can be nonzero, but since this matrix is antisymmetric the 2, 2 element must also vanish and T_1 must be zero identically. This implies $\alpha_1 = 0$, hence $G_{12} = 0$.

²The name “circular orthogonal ensemble” (COE) might be more appropriate for the ensemble of uniformly distributed orthogonal matrices, but this name is already in use for the ensemble of unitary symmetric matrices.

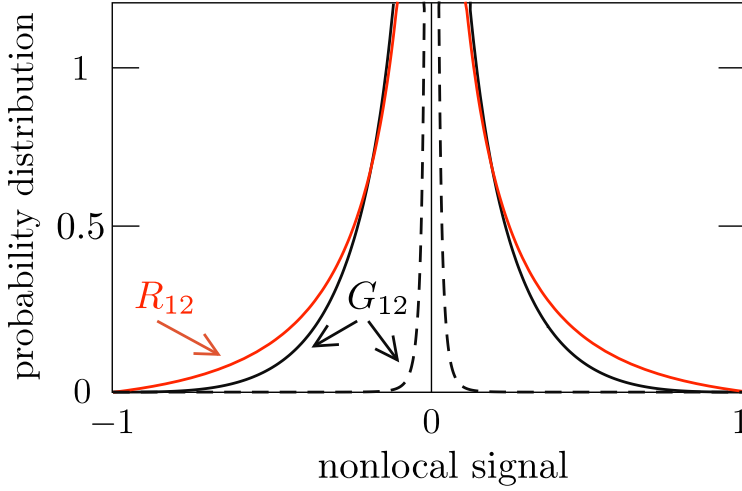


Figure 9.2: Solid curves: probability distributions of the nonlocal conductance G_{12} (in units of e^2/h) and nonlocal resistance R_{12} (in units of h/e^2). These are results for a random distribution of the 4×4 orthogonal scattering matrices S_1 and S_2 . The dashed curve shows the narrowing effect on $P(G_{12})$ of a tunnel barrier in both contacts (tunnel probability $\tau = 0.1$). In contrast, $P(R_{12})$ is not affected by a tunnel barrier.

couple electrons and holes drops out of the nonlocal resistance R_{12} . This remarkable fact is again a consequence of the product rule (9.16), which allows to factor a series conductance into a product of conductances. A tunnel barrier in contact i then appears as a multiplicative factor in α_i and G_i , and thus drops out of the ratio $\beta_i = \alpha_i/G_i$ determining R_{12} .

To demonstrate the effect of a tunnel barrier (tunnel probability τ), we have calculated the distribution of α using the Poisson kernel of the CRE [205], with the result

$$P(\alpha, \tau) = \frac{\tau^2}{[\tau + (1 - \tau)|\alpha|]^3} - \frac{\tau^2|\alpha|}{[\tau + (1 - \tau)\alpha^2]^2}. \quad (9.20)$$

The distribution of β remains given by Eq. (9.18), independent of τ . The dashed curves in Fig. 9.2 show how the resulting distribution of the nonlocal conductance becomes narrowly peaked around zero for small τ , in contrast to the distribution of the nonlocal resistance.

9.3 Discussion

Among the various candidate systems for chiral p -wave superconductivity, the recent proposal [131] based on the proximity effect in a semiconducting two-dimensional electron gas seems particularly promising for our purpose. Split-gate quantum point con-

tacts (fabricated with well-established technology) could serve as single-mode injector and detector of electrical current. The chirality of the superconducting domains is determined by the polarity of an insulating magnetic substrate, so the location of the domain wall could be manipulated magnetically. The appearance of a nonlocal signal between the two point contacts would detect the domain wall and the disappearance upon interchange of injector and detector would demonstrate the chirality.

As a direction for further research, we note that domains of opposite chirality are formed spontaneously in disordered samples. Since, as we have shown here, domain walls may carry electric current, a network of domain walls contributes to the conductivity and may well play a role in the anomalous (parity violating) current-voltage characteristic reported recently [206].

9.A Averages over the circular real ensemble

To calculate the distributions (9.18) of the parameters α_i and β_i we need the probability distribution of the 4×4 scattering matrix S_i of contact $i = 1, 2$ in the CRE. We may either work in the basis of electron and hole states, as in Ref. [204], or in the basis of Majorana states. Here we give a derivation of Eq. (9.18) using the latter basis (which is the basis we used in the main text).

A 4×4 orthogonal scattering matrix has the polar decomposition

$$S = \begin{pmatrix} e^{i\phi_1\sigma_y} & 0 \\ 0 & e^{i\phi_2\sigma_y} \end{pmatrix} \begin{pmatrix} S & C \\ (-1)^{p+1}C & (-1)^p S \end{pmatrix} \begin{pmatrix} e^{i\phi_3\sigma_y} & 0 \\ 0 & e^{i\phi_4\sigma_y} \end{pmatrix}, \quad (9.21)$$

$$C = \begin{pmatrix} \cos \psi_1 & 0 \\ 0 & \cos \psi_2 \end{pmatrix}, \quad S = \begin{pmatrix} \sin \psi_1 & 0 \\ 0 & \sin \psi_2 \end{pmatrix}, \quad (9.22)$$

in terms of six real angles. We need the uniform measure on the orthogonal group, which defines the probability distribution in the circular real ensemble (CRE). This calculation proceeds along the same lines as in Ref. [204] (where a different parametrization, in the electron-hole basis, was used). The result is that the angles $\phi_1, \phi_2, \phi_3, \phi_4$ are uniformly distributed in $(0, 2\pi)$, while the angles ψ_1, ψ_2 have the distribution

$$P(\psi_1, \psi_2) = \frac{1}{4} |\cos^2 \psi_1 - \cos^2 \psi_2|, \quad 0 < \psi_1, \psi_2 < \pi. \quad (9.23)$$

We can now obtain the joint distribution $P(\alpha_i, G_i)$ of the injection (or detection) efficiency α_i and the (dimensionless) contact conductance G_i of contact i . (We drop the label i for ease of notation.) By definition,

$$\alpha = \frac{1}{2} \text{Tr} t \sigma_y t^T \sigma_y = \cos \psi_1 \cos \psi_2, \quad (9.24)$$

$$G = 1 - \frac{1}{2} \text{Tr} r \sigma_y r^T \sigma_y = 1 - \sin \psi_1 \sin \psi_2. \quad (9.25)$$

Notice the trigonometric inequality

$$0 \leq |\alpha| \leq G \leq 2 - |\alpha|. \quad (9.26)$$

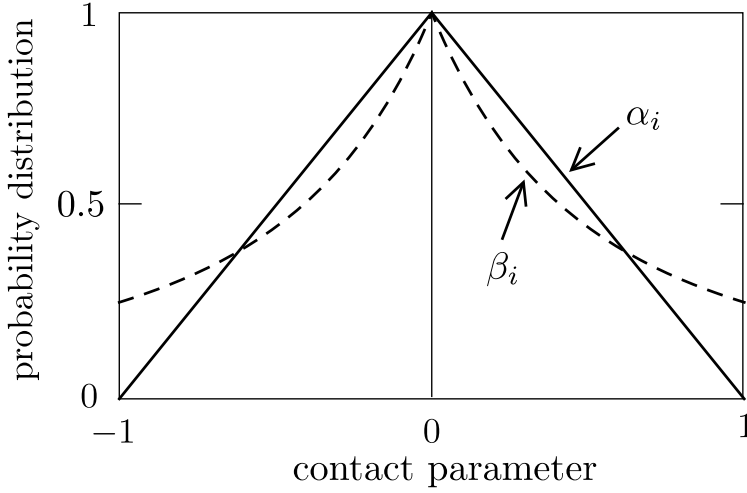


Figure 9.3: Probability distributions of the parameters α_i and $\beta_i = \alpha_i/G_i$ that characterize a single-mode contact in the CRE, given by Eqs. (9.28) and (9.30). The distribution (9.29) of $G_i - 1$ is the same as that of α_i , but these two quantities are not independent because of the inequality (9.26).

By averaging over the CRE we find, remarkably enough, that the joint distribution of α and G is uniform when constrained by this inequality,

$$\begin{aligned}
 P(\alpha, G) &= \int_0^\pi d\psi_1 \int_0^\pi d\psi_2 P(\psi_1, \psi_2) \\
 &\quad \times \delta(\alpha - \cos \psi_1 \cos \psi_2) \delta(G - 1 + \sin \psi_1 \sin \psi_2) \\
 &= \begin{cases} 1/2 & \text{if } 0 \leq |\alpha| \leq G \leq 2 - |\alpha|, \\ 0 & \text{elsewhere.} \end{cases} \quad (9.27)
 \end{aligned}$$

The marginal distributions of α , G , and $\beta = \alpha/G$ now follow by integration over $P(\alpha, G)$,

$$P(\alpha) = 1 - |\alpha|, \quad |\alpha| < 1, \quad (9.28)$$

$$P_G(G) = 1 - |G - 1|, \quad 0 < G < 2, \quad (9.29)$$

$$P(\beta) = (1 + |\beta|)^{-2}, \quad |\beta| < 1, \quad (9.30)$$

in accord with Eq. (9.18). We have plotted these distributions in Fig. 9.3.

9.B Proof that the tunnel resistance drops out of the nonlocal resistance

According to Eq. (9.17), the nonlocal conductance G_{12} is determined by the product of the injection efficiency α_1 of contact N_1 and the detection efficiency α_2 of contact N_2 . A tunnel barrier between the metal electrode and the superconductor suppresses the injection/detection efficiencies and thereby suppresses the nonlocal conductance.

The nonlocal resistance R_{12} is determined by the ratio α_i/G_i of the injection/detection efficiency and the contact conductance G_i . Since both α_i and G_i are suppressed by a tunnel barrier, one might hope that R_{12} would remain of order e^2/h . In this Appendix we investigate the effect of a tunnel barrier on the nonlocal resistance, and demonstrate that it drops out identically for a single-mode contact between the normal metal and the superconductor.

The key identity that we will use to prove this cancellation, is the product rule (9.16) and two corollaries:

$$\frac{1}{2} \text{Tr} \left(\prod_i M_i \right) \sigma_y \left(\prod_i M_i \right)^T \sigma_y = \prod_i \left(\frac{1}{2} \text{Tr} M_i \sigma_y M_i^T \sigma_y \right), \quad (9.31a)$$

$$\frac{1}{2} \text{Tr} (M \sigma_y M^T \sigma_y)^{-1} = \left[\frac{1}{2} \text{Tr} M \sigma_y M^T \sigma_y \right]^{-1}, \quad (9.31b)$$

valid for arbitrary 2×2 matrices M_i .

Considering any one of the two contacts, we assume that its scattering matrix S_0 is modified by a tunnel barrier with scattering matrix δS . Transmission and reflection submatrices are defined as in Eq. (9.8),

$$S_0 = \begin{pmatrix} r_0 & t_0 \\ t'_0 & r'_0 \end{pmatrix}, \quad \delta S = \begin{pmatrix} \delta r & \delta t \\ \delta t' & \delta r' \end{pmatrix}. \quad (9.32)$$

For a single-mode contact, each submatrix has dimension 2×2 . Both S_0 and δS are real orthogonal matrices at zero energy (in the basis of Majorana fermions). The tunnel barrier does not couple electrons and holes, which means that the submatrices of δS must commute with σ_y ,

$$[\sigma_y, \delta r] = [\sigma_y, \delta r'] = [\sigma_y, \delta t] = [\sigma_y, \delta t'] = 0. \quad (9.33)$$

The submatrices of S_0 are not so constrained.

The total scattering matrix S of the contact is constructed from S_0 and δS , according to the composition rule for scattering matrices. The transmission and reflection submatrices of S take the form

$$t = t_0 (1 - \delta r r'_0)^{-1} \delta t, \quad (9.34a)$$

$$t' = \delta t' (1 - r'_0 \delta r)^{-1} t'_0, \quad (9.34b)$$

$$r' = \delta r' + \delta t' r'_0 (1 - \delta r r'_0)^{-1} \delta t, \quad (9.34c)$$

$$r = r_0 + t_0 \delta r (1 - r'_0 \delta r)^{-1} t'_0. \quad (9.34d)$$

The injection efficiency α and detection efficiency α' are defined by

$$\alpha = \frac{1}{2} \text{Tr} t \sigma_y t^T \sigma_y, \quad \alpha' = \frac{1}{2} \text{Tr} t' \sigma_y t'^T \sigma_y. \quad (9.35)$$

Using the identities (9.31a) and (9.31b) we can factor these quantities,

$$\alpha = \alpha_0 \delta \alpha / X, \quad \alpha' = \alpha'_0 \delta \alpha' / X, \quad (9.36)$$

into the product of the injection/detection efficiencies α_0, α'_0 without the tunnel barrier and terms containing the effect of the tunnel barrier:

$$\alpha_0 = \frac{1}{2} \text{Tr} t_0 \sigma_y t_0^T \sigma_y, \quad \alpha'_0 = \frac{1}{2} \text{Tr} t'_0 \sigma_y t'^0_T \sigma_y, \quad (9.37a)$$

$$\delta \alpha = \frac{1}{2} \text{Tr} \delta t \sigma_y \delta t^T \sigma_y, \quad \delta \alpha' = \frac{1}{2} \text{Tr} \delta t' \sigma_y \delta t'^T \sigma_y, \quad (9.37b)$$

$$X = \frac{1}{2} \text{Tr} (1 - \delta r r'_0) \sigma_y (1 - \delta r r'_0)^T \sigma_y. \quad (9.37c)$$

Since δt and $\delta t'$ commute with σ_y , the terms $\delta \alpha, \delta \alpha'$ simplify to

$$\delta \alpha = \delta \alpha' = \frac{1}{2} \text{Tr} \delta t \delta t^T, \quad (9.38)$$

where we have used the orthogonality condition, $\delta S^T \delta S = \delta S \delta S^T = 1$, to equate the traces of $\delta t \delta t^T$ and $\delta t' \delta t'^T$. The term X can similarly be reduced to

$$X = 1 + (1 - \delta \alpha)(1 - G_0) - \text{Tr} \delta r r'_0, \quad (9.39)$$

where G_0 is the contact conductance (in units of e^2/h) in the absence of the tunnel barrier:

$$G_0 = \frac{1}{2} \text{Tr} (1 - r'_0 \sigma_y r_0^T \sigma_y). \quad (9.40)$$

We now turn to the contact conductances G_i , in order to show that the effect of the tunnel barrier is contained in the same factor $\delta \alpha / X$ (which will then cancel out of the ratio $\beta_i = \alpha_i / G_i$). Considering again a single contact, and dropping the index i for ease of notation, we start from the definition of the contact conductance (in units of e^2/h):

$$G = \frac{1}{2} \text{Tr} (1 - r' \sigma_y r'^T \sigma_y). \quad (9.41)$$

We substitute Eq. (9.34c), and try to factor out the terms containing the transmission and reflection matrices of the tunnel barrier.

It is helpful to first combine the two terms in Eq. (9.34c) into a single term, using the orthogonality of δS :

$$\begin{aligned} r' &= -(\delta t'^T)^{-1} \delta r^T \delta t + \delta t' r'_0 (1 - \delta r r'_0)^{-1} \delta t \\ &= (\delta t'^T)^{-1} (r'_0 - \delta r^T) (1 - \delta r r'_0)^{-1} \delta t. \end{aligned} \quad (9.42)$$

We now substitute Eq. (9.42) into Eq. (9.13) and use the identities (9.31) to factor the trace,

$$\begin{aligned} G &= 1 - X^{-1} \frac{1}{2} \text{Tr} (r'_0 - \delta r^T) \sigma_y (r_0^T - \delta r) \sigma_y \\ &= 1 - X^{-1} (2 - \delta \alpha - G_0 - \text{Tr} \delta r r'_0), \end{aligned} \quad (9.43)$$

where we also used the commutation relations (9.33). The remaining trace of $\delta r r'_0$ can be eliminated with the help of Eq. (9.39), and so we finally arrive at the desired result:

$$G = G_0 \delta \alpha / X. \quad (9.44)$$